Proceedings of the 6th World Congress on Momentum, Heat and Mass Transfer (MHMT'21)
~~Lisbon, Portugal~~ Virtual Conference– June 17 – 19, 2021
Paper No. ENFHT 306
DOI: 10.11159/enfht21.lx.306

Numerical Modelling Of a Rectangular Shell-And-Tube Heat Exchanger

Marwa Ben Slimene[1,*], Sébastien Poncet[2], Jamel Bessrour[1], Ftouh Kallel[3]
[1]Mechanical Engineering Department, National Engineering School of Tunis
BP37, El Belvedere 1002, Tunis, Tunisia
*marwa-benslimene@outlook.com
[2]Mechanical Engineering Department, Université de Sherbrooke
2500 boulevard de l'Université, Sherbrooke (QC) J1K 2R1, Canada
[3]Energetic Engineering Department, Private University of Tunis
30 Av. Kheireddine Pacha 1002, Tunis, Tunisia

Abstract - Numerical simulations have been carried out to investigate the turbulent flows and coupled conductive/convective heat transfers in a glycol to water shell-and-tube heat exchanger (one shell, one tube and six passes). The refrigerant (glycol) flows in the tube, and a secondary fluid (water) flows in the shell. The k-ω SST model is used to close the system of equations in the turbulent regime. The present model is first favorably compared and validated against experimental and numerical data available in the literature. It is then extended to consider the shell-and-tube configuration with a rectangular shell. Its thermo-hydraulic performances in the tube side are quantified for Reynolds numbers ranging from 1.03×10^3 to 1.47×10^5. The performance of the heat exchanger is then enhanced by introducing baffles in the shell. The results are finally compared and discussed in terms of three global performance metrics.

***Keywords*:** RANS modeling, shell-and-tube heat exchanger, rectangular shell, baffles.

1. Introduction

Heat exchangers are widely used in many engineering applications such as for heating/cooling, refrigeration or air conditioning systems, thermal energy storage systems, chemical industries and power generation in large thermal plants, and so on. The heat exchanger design depends on the targeted applications. The most common ones are the heat pipes exchangers [1], helical coil and straight tube heat exchangers [2], plate heat exchangers [3], etc. One of the most used types of heat exchangers in the process or food industries is the shell and tube heat exchanger (STHE) because of its versatility, robustness, easy maintenance and possible geometrical improvements. STHEs have besides 40% share apparatus of the different industry as stated by Arani and Moradi [4]. The literature review demonstrates that most works focused on STHEs having a cylindrical cross-section on the shell side. Such STHEs have some limitations due to the cylindrical shell geometry: a limited number of possible shell pass (maximum two passes as recommended by [5]), a complete counter flow cannot be achieved, the working space requirement is usually larger compared to their rectangular counterpart, etc. Huge research efforts have been made during the past decades to improve their thermo-hydraulic performances by introducing baffles (segmental, helical, inclined), fins of different geometries along the tubes or the shell or by changing the tube configuration and their arrangement. Though they drastically increase the effectiveness of STHE, baffles introduce problems commonly encountered in prototypes: increased pressure drop, decreased lifetime due to vibrations and fouling.

Due to the large number of degrees of freedom (geometrical parameters, operating conditions), many researches recently focused on the design optimization of STHE with improved effectiveness and reduced capital cost as objective functions. Bicer et al. [6] combined a CFD analysis using the standard k-ε model and the Taguchi method to investigate various shapes of baffles for STHE. Three-zonal baffles exhibited the lowest pressure drop while keeping high thermal performances.

Computational Fluid Dynamics (CFD) simulations remain a valuable tool to investigate in details the fluid flow and heat transfer in STHE before improving their design. However, most of the time, authors prefer to increase the design complexity by increasing the number of tubes or introducing innovative baffle geometries, to the detriment of a well-captured near-wall modeling and computational efforts and of a global validation. Sometimes, no validation is provided as for Foster et al. [7], who modeled a fractal branch-like STHE without besides mentioning the applied turbulence closure. Most of the time, high Reynolds number approaches based on a k-ε model with wall function are preferred. As an example, Arani and Moradi [4] optimized a SHTE with segmental baffles using the SolidWorks Flow Simulation. They considered a standard k-ε model

with wall function without precising the mesh grid. They validated their approach in terms of pressure drop and shell-side heat transfer coefficient for three operating conditions, getting a maximum discrepancy of 24%. Tuncer et al. [8] investigated the influence of longitudinal fins on the performance of a shell and helically coiled tube heat exchanger using a RNG k-ε model. The benefit from using fins is of the same order as the discrepancy between their CFD and experimental results. Liu et al. [9] compared three turbulence models, namely the RNG and realizable k-ε and k-ω SST models for a STHE with baffles. Surprisingly, the latter model performs worst but it has to be noticed that the mesh grids and wall resolutions are not provided. The same mesh grid has been probably used but then, no definitive conclusion can be done. Alimoradi et al. [10] were one of the few authors to perform large eddy simulations for a shell and coiled tube heat exchanger with fins on the external wall of the tube. LES were compared to the realizable k-ε and k-ω models for three cases at a fixed spatial resolution. However, as the wall resolution is not mentioned, it was surprising to obtain indistinguishable results.

The literature on STHE with a rectangular cross-section on the shell side is scarce. Patel et al. [11] addressed the weakness of the conventional SHTE with a cylindrical shell. They designed a new experimental set-up with a rectangular shell. Besides the facts that it provides the flexibility to increase the number of shell pass and a complete counter flow may be achieved, this novel shell geometry provided, for the same heat transfer rates, an enhanced Effective Mean Temperature Difference and less heat surface area compared to cylindrical STHE.

2. Numerical Modeling

2.1. Geometrical Modeling

Figure 1 presents a shell-and-tube heat exchanger composed of one rectangular shell in which the fluid does one pass and one tube doing six passes. The hot fluid is water and flows within the tank through three tubes at inlet velocity V_h=1 m/s and temperature T_h=14ºC. It corresponds to a Reynolds number Re_h=60 545 based on the tube diameter D_h. On the tube side, glycol flows through a stainless steel pipe of diameter D_c =48.2 mm at an inlet velocity V_c, which varies between 0.7 and 10 m/s and an inlet temperature T_c=8ºC. So the Reynolds number for the glycol flow Re_c varies between 10 292 and 147 034. Five rectangular baffles alternatively placed along the top and bottom walls of the shell may be added to increase its performance. The properties of fluids and steel are given in Table 1, while Table 2 lists the geometrical parameters.

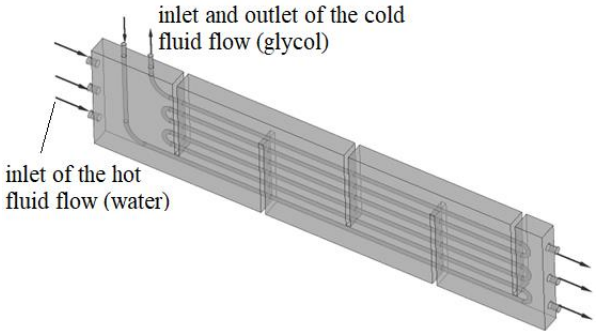

Fig. 1: Schematic view of the shell-and-tube heat exchanger with baffles

Table 1: Thermophysical properties of materials. Note that the fluid properties are evaluated at their corresponding inlet temperatures.

	Water	Glycol	Steel
Density ρ (kg.m^{-3})	999	1057	7854
Specific heat capacity Cp (J.kg^{-1}.K^{-1})	4181.7	3611	434
Thermal conductivity λ (W.m^{-1}.K^{-1})	0.6069	0.464	60.5
Dynamic viscosity μ (Pa.s)	1.32×10^{-3}	3.465×10^{-3}	-

Table 2: Geometrical characteristics of the heat exchanger.

Parameters	Values	Parameters	Values
Width of the shell [mm]	1200	Pitch of the tube [mm]	750
Length of the shell [mm]	5000	Number of tubes [mm]	1
Inlet and outlet diameters of the shell tube [mm]	80	Length of the baffles [mm]	900
Outer diameter of the tube [mm]	48.2	Width of the baffles [mm]	5
Thickness of the tube wall [mm]	5	Spacing between two baffles [mm]	900
Effective length of the tube [mm]	4200	Number of baffles	5

2.2. Numerical method

The numerical computations are carried out by solving the governing differential equations for the conservation of mass, momentum and energy in cylindrical coordinates (r,θ,z). The fluids are assumed to be Newtonian and incompressible.

The CFX 17.1 solver available in ANSYS Workbench 17 based on the finite volume method is used. Second-order upwind schemes are employed for the spatial discretization. The SIMPLE algorithm enables to overcome the velocity-pressure coupling. All gradients are evaluated using the least squares cell-based method.

As shown in the following section, the temperature gradients are relatively weak such that the Boussinesq approximation remains valid in both cases. In the turbulent regime, the Shear Stress Transport (SST) k-ω model proposed by Menter [12] is preferred. It combines the robust and accurate formulation of the k-ω in the near wall region and the free stream independence of the k-ε outside. Blending functions are introduced in the transport equation of k and ω. Sekrani et al. [13] demonstrated its superiority over other two-equation closure and also over Reynolds Stress Models for a turbulent heated pipe flow, which confirmed the former results of Pal et al. [14] for a STHE with tube bundle. Convergence of the solution is achieved when all the residuals are less than 10-5 and the mass flow rate is conserved at +/- 0.1%.

2.3. Boundary conditions and mesh grid

Prescribed velocity and temperature are imposed at all inlets. The mean inlet velocity and temperature imposed at the shell side are fixed to V_h=1 m/s and T_h=14ºC, respectively, in all calculations. At the pipe inlet, the averaged velocity V_c is varied between 0.7 and 10 m/s, while temperature remains constant (T_c=8ºC). A turbulent intensity of 5% is imposed at all inlets but results showed that the flow field and heat transfer are not sensitive to that parameter. A pressure boundary condition is prescribed at both outlets. No slip wall boundary conditions are adopted on all walls. The shell and its inlet and outlet pipes are assumed as adiabatic. Note also that conductive heat transfer within the pipe wall is accounted for.

A mesh grid with tetrahedral elements is used for the rectangular shell-and-tube heat exchanger. It consists of 11.85 millions of elements on the hot fluid side (shell), 1.47 millions of elements on the cold fluid side (tube) and 0.45 million of elements for the solid tube walls for the case without baffles, leading to a maximum wall coordinate y+ equal to 1.68 in the tube. For all calculations, the associated computational time step is fixed to 10-3 s.

2.4. Validation

The present solver is validated regarding the counter current double tube pass shell and tube heat exchanger (DTP-STHE) with segmental baffles considered experimentally and numerically by He and Li [15]. The inlet mass flow rate varies between 1.1 and 1.9 kg/s at the inlet of the shell side with a temperature fixed to 353.15 K. The mass flow in the tubes is set to 0.2 kg/s with a temperature of 293.15 K. The working fluid is water for both shell and tubes.

Figure 2a displays the variation of the heat transfer coefficient on the shell side as a function of the Reynolds number based on the mass flow rate imposed at the shell inlet. The present CFD results are compared to the experimental data of He and Li [15] and their numerical predictions using a RNG k-ε model with standard wall functions. As expected, the overall heat transfer coefficient on the shell side increases by increasing the shell Reynolds number. More interestingly, the present k-ω SST model predicts quite well the variations of the heat transfer coefficient for this range of Reynolds number. Despite some weak discrepancies, which may be in the uncertainty range of the experiments (not precised), the present model greatly improves the predictions of their RNG k-ε model. First, their mesh is slightly coarser with 4.6 millions of elements (against

5.5 millions here) but it can be mainly attributed to the poor performance of the standard wall function, whereas the thin boundary layers are accounted for here with a k-ω closure. The present CFD can be then used confidently to model the turbulent flow and associated conjugate heat transfer in a rectangular shell and tube heat exchanger.

The design of a cylindrical-shape shell leads indeed to some limitations such as, corrosion problems due to dead zones, long heat exchanger circuits for optimum conditions, high pressure drops, limited number of shell passes, working volume and space requirement, etc [5]. A rectangular shell provides the flexibility to increase the number of shell passes and a complete counter flow can be achieved due to the rectangular form of the shell. While a maximum of two shell passes are possible for a cylindrical STHE, the number of shell passes for a rectangular STHE may be equal to the number of tube passes. The objective of the present study is then to characterize the performance of a rectangular STHE.

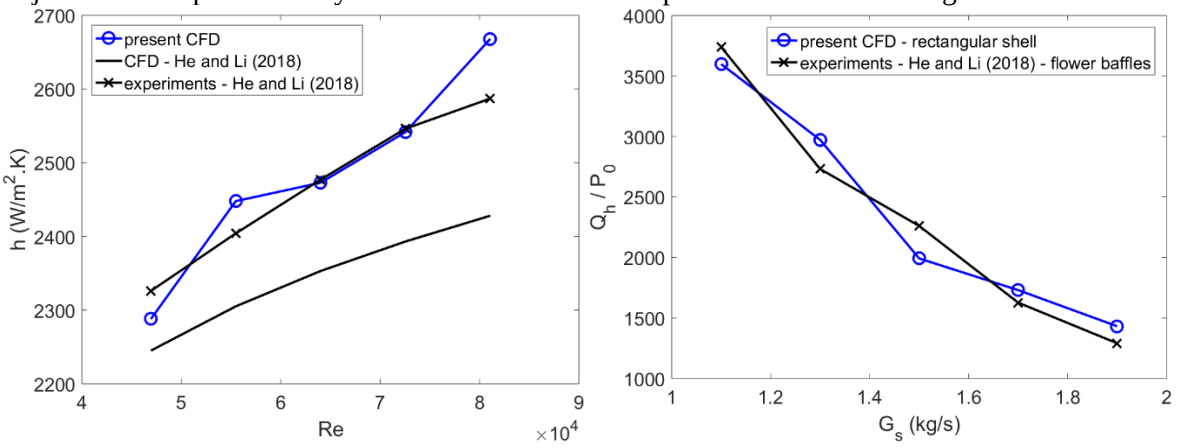

(a) (b)

Fig. 2: Comparison with He and Li [15] for a shell and tube heat exchanger: (a) Variations of the shell side heat transfer coefficient versus the Reynolds number; (b) Variations of the heat transfer rate Q_h per effective pumping power P_0 versus the mass flow rate G_s in the shell (flower baffles).

Figure 2b displays the evolution of the heat transfer rate Qh per effective pumping power P0 as a function of the mass flow rate Gs on the shell side. The present results obtained for a rectangular STHE are compared to the experimental data of He and Li [15] for a double-tube-pass STHE equipped with flower baffles. Both shells have the same length (500 mm) and the width of the rectangular one is equal to the diameter (87 mm) of the cylindrical one to keep the same overall volume required to install the heat exchanger. All operating parameters are set to the same values between the two configurations. He and Li [15] demonstrated that such baffles lead to better overall performance compared to helical and segmental baffles. It can be seen that these two shell geometries lead to similar values of Qh / P0 for this range of Gs values. The present results confirm then that a rectangular shell leads to improved overall performance compared to their cylindrical counterpart.

3. Results and discussion

3.1. Mean flow and thermal fields

The variations of the average friction factor for the refrigerant fluid on the tube side as a function of the pipe Reynolds number are assessed by comparing the predictions of both shell and tube heat exchanger with and without baffles. The average friction factor Cf,c obtained by the present model is compared to the Blasius law for turbulent pipe flows given by:

$$C_{f,c} = \frac{8\tau_{m,c}}{\rho {V_c}^2} = 0.316 \times Re_c^{-0.25} \quad (1)$$

with $\tau_{m,c}$ the mean shear stress at the tube wall. The distributions of the friction factor for both configurations with and without baffles as a function of the Reynolds number in the tube are shown in Figure 3a. A reasonable agreement between the numerical results and theoretical values calculated using the Blasius equation is observed. The friction factor decreases

with increasing Re_c for the cases with and without baffles. The wall shear stress increases then slower than the inlet velocity. However, the configuration with baffles provides higher values of the friction factor compared to the case without baffles.

Figure 3b displays the variations of the Nusselt number on the tube side Nuc as a function of the inlet Reynolds number Rec with and without baffles. As expected, the Nusselt number increases with increasing Reynolds number. It can be noticed that it increases very slowly for the case without baffles reaching almost an asymptotical value close to Nuc=120 at 1.47×105. With baffles, Nuc increases much faster. Baffles play their role by enhancing the mixing in the shell and then increasing the heat transfer rate with the pipe. The enhancement ratio ER (the ratio between the Nuc values with and without baffles) varies from 2.33 and 2.75 for this range of Rec values, with an average value of ER=2.64.

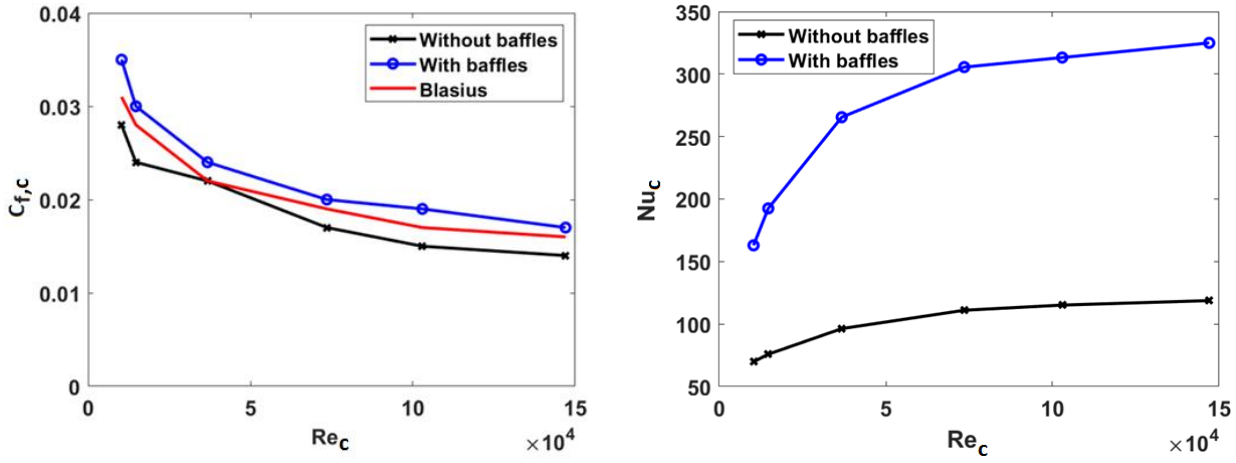

(a) (b)

Fig. 3: Variations of the (a) friction faction and the (b) Nusselt number as a function of the pipe Reynolds number.

The preponderant influence of the five rectangular baffles is confirmed by looking at the temperature contours in the medium plane of the shell, as displayed in Figure 4. One recalls that the inlet velocity imposed in the three inlet tubes of the shell for the hot fluid (water) is fixed to V_h=1 m/s. At Re_c=1.47×10^4, temperature is almost homogeneously distributed within the shell with a temperature difference for the shell side of only $\Delta T_h = 0.23$ K for the case without baffle. By increasing the pipe Reynolds number by a factor of 10, this temperature difference increases slightly up to 0.7 K. By adding baffles in the shell, ΔT_h increases from 2.2 K at Re_c=1.47×10^4 to 6.6 K at 1.47×10^5.

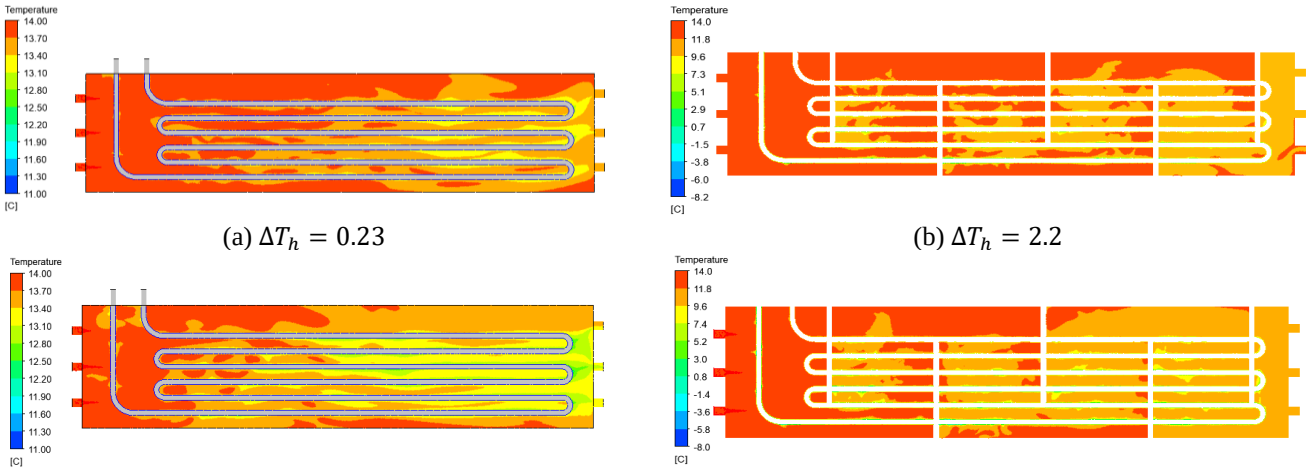

(a) $\Delta T_h = 0.23$ (b) $\Delta T_h = 2.2$

(c) $\Delta T_h = 0.45$ (d) $\Delta T_h = 2.78$

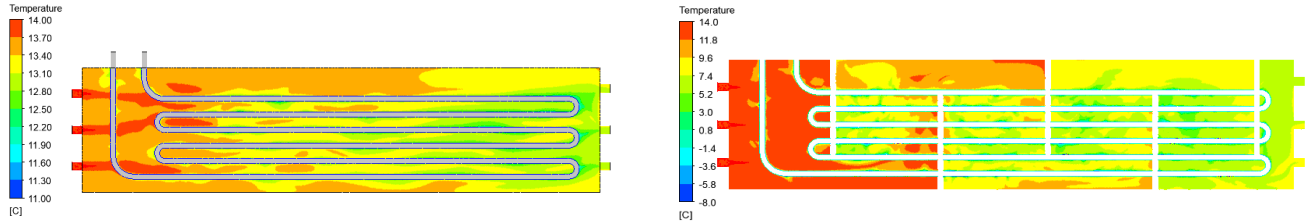

(e) $\Delta T_h = 0.7$ (f) $\Delta T_h = 6.6$

Fig. 4: Temperature contours in the medium plane of the shell for three values of the pipe Reynolds number: (a,b) $Re_c = 1.47\times10^4$, (c,d) $Re_c = 7.35\times10^4$ and (e,f) $Re_c = 1.47\times10^5$. Results obtained without (a,c,e) and with (b,d,f) baffles.

On Figures 4d and 4f, it is clear that the five baffles enhance mixing by affecting the mean flow between successive baffles. It can be seen more clearly by looking at the streamline patterns colored by the velocity magnitude displayed in Figure 5 for Rec=7.35×104. For the case without baffle (Fig.5a), the streamlines are almost horizontal from the inlet tubes to the outlet ones, being only slightly disturbed by local turbulence and weak recirculations. For the case with five rectangular baffles (Fig.5b), the flow velocity increases in the region between the edge of the first baffle and the bottom of the shell, as the fluid passage area is decreased. The fluid then impinges the second baffle (placed in a staggered arrangement), is deflected upwards, flows along this second baffle, impinges the top wall of the shell, so on and so forth. It creates a large recirculation zone at the back of the first baffle. The combination of higher local velocity (higher local Reynolds number) and large recirculation zones, which increase thermal mixing, is highly favorable for the heat transfer.

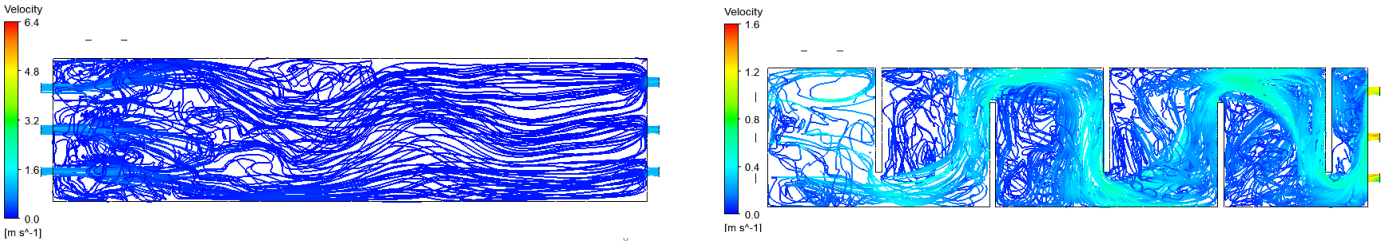

(a) (b)

Fig. 5: Streamlines colored by the velocity magnitude in the medium plane of the shell: (a) without baffles; (b) with baffles. Results obtained for $Re_c = 7.35\times10^4$

3.2. Performance criteria

The results are discussed here in terms of three global performance criteria. The PEC number is defined as the ratio of heat flow rate transferred to the required pumping power [13]:

$$\mathrm{PEC} = \frac{\dot{m}_c C_{p,c} \Delta T_c}{\dot{V}_c \, \Delta p_c} \tag{2}$$

where $\dot{m}_c$ and $\dot{V}_c$ are the mass and volumetric flow rates within the tube, respectively, ΔT_c and Δp_c are the temperature and pressure differences between the outlet and the inlet of the tube.

The field synergy number Fc on the tube side may be employed for quantifying the field synergy between the velocity and temperature fields. Fc stands for the dimensionless heat source strength over the entire convection domain. It writes [16]:

$$Fc = \frac{Nu_c}{Re_c \, Pr_c} \tag{3}$$

The effectiveness of the heat exchanger ε is defined as:

$$\varepsilon = \begin{Bmatrix} (T_{h,i} - T_{h,o})/(T_{h,i} - T_{c,i}) \text{ if } \min(\dot{m}\mathrm{Cp}) = (\dot{m}\mathrm{Cp})_h \\ (T_{c,o} - T_{c,i})/(T_{h,i} - T_{c,i}) \text{ if } \min(\dot{m}\mathrm{Cp}) = (\dot{m}\mathrm{Cp})_c \end{Bmatrix} \tag{4}$$

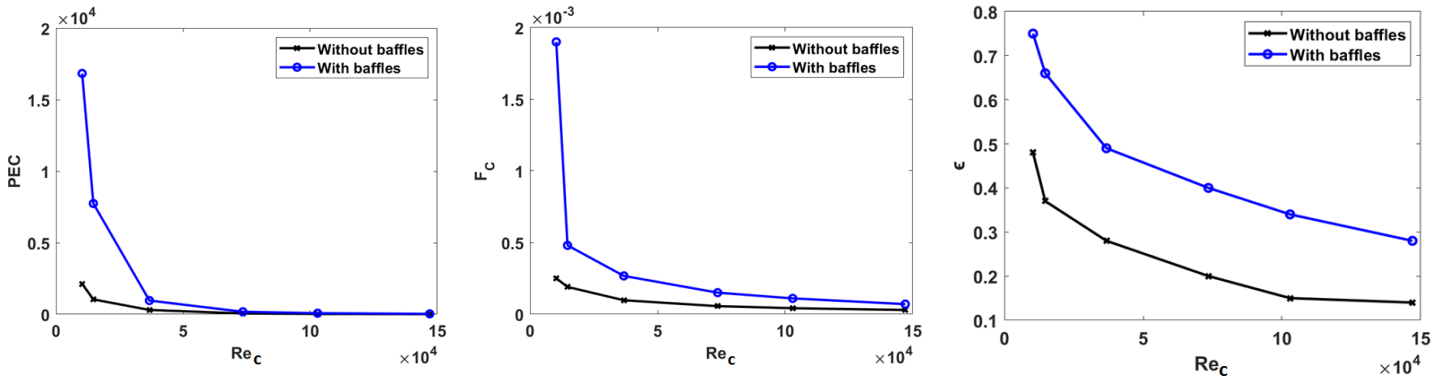

(a) (b) (c)

Fig. 6: Variations of the three performance metrics as a function of the pipe Reynolds number: (a) PEC, (b) field synergy number Fc and (c) effectiveness of the heat exchanger ε.

Figure 6a displays the PEC number as a function of the pipe Reynolds number. The presence of baffles increases the PEC number significantly, especially at lower Reynolds numbers. For both cases, PEC decreases with increasing Re_c, confirming the results of Ferrouillat et al. [17] obtained for the heat transfer of SiO_2/water nanofluids in a heated pipe.

The field synergy number Fc corresponds to the I factor introduced by Guo et al. [16]. Figure 6b displays the variations of Fc as a function of the pipe Reynolds number. For both configurations, it decreases when Re_c increases, which confirms the former results of [16] for laminar flows in various configurations including a stagnation point, a boundary layer plate flow and a duct flow. For these last geometries, Fc scales with $Re^{-1/2}$. Guo et al. [18] used this parameter based on the shell side characteristics to optimize a STHE with baffles. For a given set of operating conditions, they reported an initial value of 0.0021 (ε=0.576) and an optimal one of 0.003 (ε=0.6044). Though one considers here the Fc number for the tube side, these values are quite comparable to the maximum value obtained at the lowest Reynolds number for the case with baffles (Fig.6b).

More interestingly is the variation of the heat exchanger effectiveness as a function of the pipe Reynolds number displayed in Figure 6c. As expected, the effectiveness decreases by increasing the pipe Reynolds number, its maximum value being reached at $Re_c=1.47\times10^3$. This is a direct consequence of its definition, which is the ratio of temperature difference of minimum heat capacity fluid to the temperature difference between the two inlets. At a given Reynolds number $Re_c=1.47\times10^3$, the presence of baffles increases ε from 49% to about 76%. Though the operating conditions are different, two interesting points have to be noticed: (1) the maximum effectiveness is achieved when the other metrics are maximum too, confirming the results of Guo et al. [18]; (2) the present heat exchanger is more efficient than the optimal one (cylindrical shell) proposed by [18], while the synergy field number remains always lower than in their case. It may lead to two conclusions: Fc may be not the most reliable metrics to characterize the heat exchanger performance. The second conclusion is that this last result confirms that rectangular shells are usually more efficient than their cylindrical counterpart.

4. Conclusion

Turbulence modelling using a k-ω SST closure has been carried to study the turbulent flow and coupled heat transfer in a rectangular shell and tube heat exchanger. The numerical solver has been first validated for a double tube pass STHE with baffles studied experimentally by He and Li [15]. A very close agreement was obtained, the present k-ω SST improving besides the predictions of the RNG k-ε model. The most interesting feature was that the rectangular cross-section of the shell enabled to get the same performance as the optimal heat exchanger equipped with flower baffles proposed by [15].

The calculations have been then extended to the case of an industrial shell and tube heat exchanger (one rectangular shell, one tube with six passes). The glycol Reynolds number in the tube side has been varied from 1.03×10^3 to 1.47×105. The maximum effectiveness ε=0.76 was obtained at the lowest Reynolds number for a shell equipped with baffles. Baffles enable to increase the residence time of the hot fluid in the shell while inducing large recirculations, which improve mixing. Though the PEC number led to similar conclusions, the field synergy number appeared as a less reliable metrics to optimize

heat exchanger. The overall high effectiveness of the present design may be attributed here to the rectangular cross-section shell, which, by comparisons with literature data, outperforms its cylindrical counterpart.

Acknowledgements

S.P. would like to thanks the NSERC chair on industrial energy efficiency established at Université de Sherbrooke in 2019 with the financial support of Hydro-Québec, Natural Resources Canada and Emerson Residential and Commercial Solutions. The calculations have been performed using the HPC facilities of Compute Canada.

References

[1] W. Srimuang and P. Amatachaya, "A review of the application of heat pipe heat exchangers for heat recovery", *Renew. Sustain. Ener. Rev.*, vol. 16, pp.4303-4315, 2012.

[2] N.D. Shirgire and P.V. Kumar, "Review on comparative study between helical coil and straight tube heat exchanger", *J. Mech. Civil Eng.*, vol. 8, no. 2, pp.55-59, 2013.

[3] M. Abou Elmaaty, A.E. Kabeel and M. Mahgoub, "Corrugated plate heat exchanger review", *Renew. Sustain. Ener. Rev.*, vol. 70, pp.852-860, 2017.

[4] A.A.A. Arani and R. Moradi, "Shell and tube heat exchanger optimisation using new baffle and tube configuration", *Appl. Therm. Eng*, vol. 157, 113736, 2019.

[5] Tubular Exchanger Manufacturer Association (TEMA): http://www.wermac.org/equipment/heatexchanger_part5.html

[6] N. Bicer, T. Engin, H. Yasar, E. Buyukkaya, A. Aydin and A. Topuz, "Design optimization of a shell-and-tube heat exchanger with novel three-zonal baffle by using CFD and taguchi method", *Int. J. Therm. Sci*., vol. 155, 106417, 2020.

[7] N. Foster, D. Sebastia-Saez and H. Arellano-Garcia, "Fractal branch-like fractal shell-and-tube heat exchangers: A CFD study of the shell side performance", *IFAC papersonline*, vol. 52-1, pp.100-105, 2019.

[8] A.D. Tuncer, A. Sozen, A. Khanlari, E.Y. Gürbüz and H.I. Variyenli, "Upgrading the performance of a new shell and helically coiled heat exchanger by using longitudinal fins", *Appl. Therm. Eng.*, vol. 191, 116876, 2021.

[9] Y. Liu, J. Wen, S. Wang and J. Tu, "Numerical investigation on the shell and tube heat exchanger with baffle leakage zones blocked", *Int. J. Therm. Sci.*, vol. 165, 106959, 2021.

[10] A. Alimoradi, M. Olfati and M. Maghareh, "Numerical investigation of heat transfer intensification in shell and helically coiled finned tube heat exchangers and design optimization", *Chem. Eng. Process.*, vol. 121, pp. 125-143, 2017.

[11] V. Patel, R. Patel and V. Savsani, "Novel heat exchanger design with rectangular shell geometry", In *Proceedings of the ASME 2014 International Mechanical Engineering Congress and Exposition*, Montreal, Canada, 2014.

[12] F.R. Menter, "Two-equation eddy-viscosity turbulence models for engineering applications", *AIAA J.*, vol. 32, no. 8, pp.1598–1605, 1994.

[13] G. Sekrani, S. Poncet and P. Proulx, "Modeling of convective turbulent heat transfer of water-based Al_2O_3 nanofluids in an uniformly heated pipe", *Chem. Eng. Sci.*, vol. 176, pp.205-219, 2018.

[14] E. Pal, I. Kumar, J.B. Joshi and N.K. Maheshwari, "CFD simulations of shell-side flow in a shell-and-tube type heat exchanger with and without baffles", *Chem. Eng. Sci.*, vol. 143, pp.314-340, 2016.

[15] L. He and P. Li, "Numerical investigation on double tube-pass shell-and-tube heat exchangers with different baffle configurations", *Appl. Therm. Eng*., vol. 143, pp.561-569, 2018.

[16] Z.Y. Guo, D.Y. Li and B.X. Wang, "A novel concept for convective heat transfer enhancement", *Int. J. Heat Mass Transf*., vol. 41 (14), pp.2221-2225, 1998.

[17] S. Ferrouillat, A. Bontemps, J.P. Ribeiro, J.A. Gruss and O. Soriano, "Hydraulic and heat transfer study of SiO_2/water nanofluids in horizontal tubes with imposed wall temperature boundary conditions", *Int. J. Heat Fluid Flow*, vol. 32, no. 2, pp.424-439, 2011.

[18] J. Guo, M. Xu and L. Cheng, "The application of field synergy number in shell-and-tube heat exchanger optimization design", *Appl. Ener.*, vol. 86, pp.2079-2087, 2009.